Interpretation of a Fractured Dolomite Core: Margaree F-70, Deep Panuke, Nova Scotia, Canada

Leslie Eliuk *for* **Rick Wierzbicki, Kevin Gillen, Rolf Ackermann, Nancy Harland, Leslie Eliuk, with a contribution by Jeff Dravis**

Abstract: *The purpose of this presentation is to show the facies, diagenesis, and fracture interpretation of the fractured and dolomitized margin of the Abenaki carbonate platform at Deep Panuke. Core from F-70, H-08, and PI-1B will be displayed.*

The Deep Panuke gas reservoir was discovered in 1999, 250 km offshore of Halifax Nova Scotia. Gas is trapped in dolomite and limestone at the margin edge of the Jurassic aged Abenaki carbonate complex. Analysis of well test data had indicated that platform margin edge wells were connected to a highly permeable reservoir, assumed to be fractured or vuggy dolomite/limestone.

In 2004, data was obtained on the high permeability reservoir, when 24 meters of core was recovered from the F-70 well bore. The F-70 core encountered foreslope and reefal limestone and fractured vuggy dolomite in the upper portion of the reservoir. The core was examined and facies described in detail by Les Eliuk. Thin sections were examined and a diagenetic interpretation provided by Jeff Dravis.

The core and associated FMI image from F-70 was interpreted by Kevin Gillen. Data from his interpretation and interpretation of all of the FMI data by HEF Petrophysical were used by Rolf Ackerman (Beicip Inc.) to build a discrete fracture network model of the reservoir. The parameters and insights gained have been used to constrain the flow simulation model of the reservoir.

Repeated with only minor modification by permission from Canadian Society of Petroleum Geologists 2005 Core Conference in Calgary Alberta. Additions have been made to Eliuk's section on depositional setting and that will be the emphasis of the 2008 display. Also a brief appendix has been added with information on cores from Panuke PI-1A and H-08. Panuke M-79 has a 5m core in the basal Scatarie Member rich in quartz grains and ooids that will not be shown

Introduction:

The Deep Panuke gas reservoir was discovered in 1999 with the drilling of the PP-3C exploration well from the production platform of the Cretaceous Panuke oil pool. Gas is trapped in a combined structural stratigraphic trap in Jurassic aged limestones and dolomites of the Abenaki Formation. The discovery and subsequent drilling activity have been described in Weissenberger et al (2000) and Harland et al. (2002). Weissenberger et al. (2006) gives the carbonate sequence stratigraphy and petroleum geology for Deep Panuke but due to confidentiality did not include data from Margaree F-70. More recent well data and details of planned and approved EnCana Deep Panuke field development can be accessed on the Canada-Nova Scotia Offshore Petroleum Board's website (EnCana 2006). The Abenaki Formation margin is a stacked series of coral-stromatoporoid reefs, lower energy sponge reefs, and associated carbonate ramp deposits that developed on the outer edge of the North Atlantic margin above basement horsts. The regional geology is described in Given (1977), and Wade and MacLean (1990). Facies types and distribution are described in: Wierzbicki et al 2002 which built upon the earlier work of Eliuk (1978). The Abenaki carbonates have been partially dolomitized, recrystallized, and fractured and leached. The diagenetic model is described in: Wierzbicki et al (2002, 2005 and 2006), Wierzbicki and Harland (2004) and Eliuk (1978) and (2004).

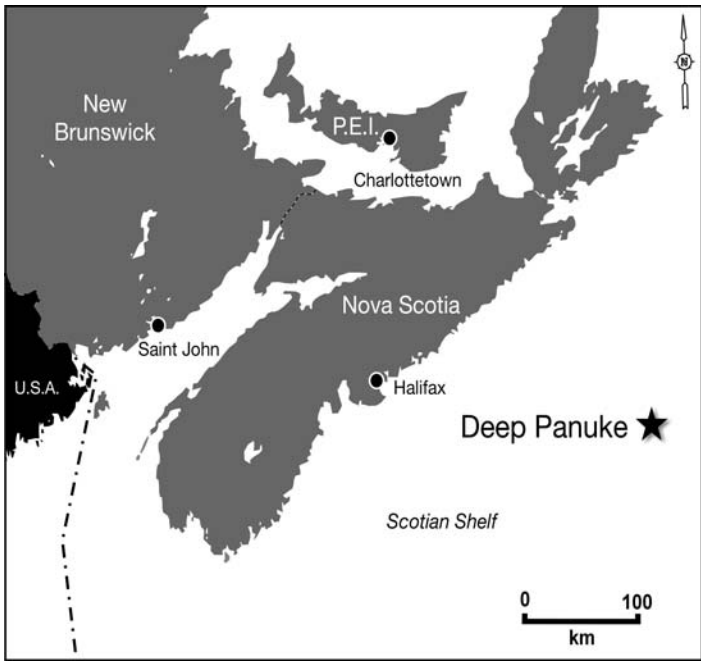

Figure 1: Location of the Deep Panuke reservoir 250 km to the ESE of Halifax, Nova Scotia.

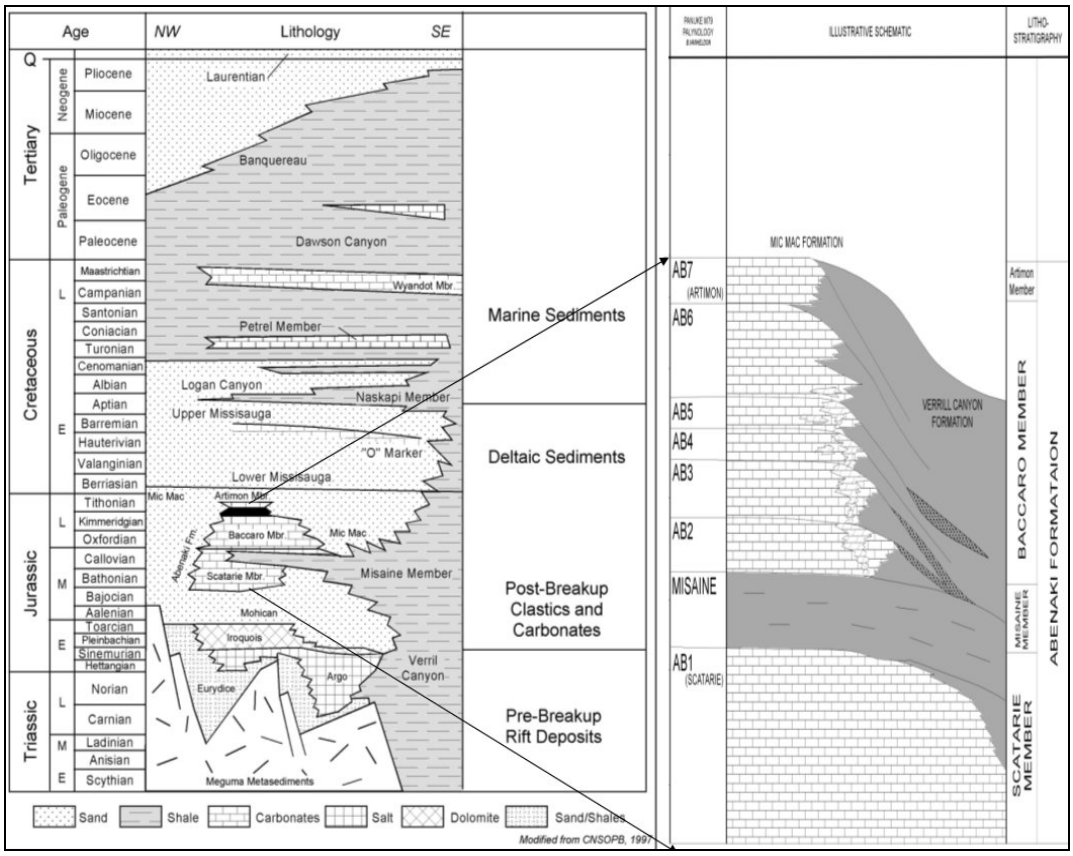

Figure 2: Offshore Nova Scotia Stratigraphy, from CNSOSPB, the Abenaki carbonate margin developed in mid-to late Jurassic between offshore shale and near shore clastics, EnCana has divided the Abenaki into 7 cycles.

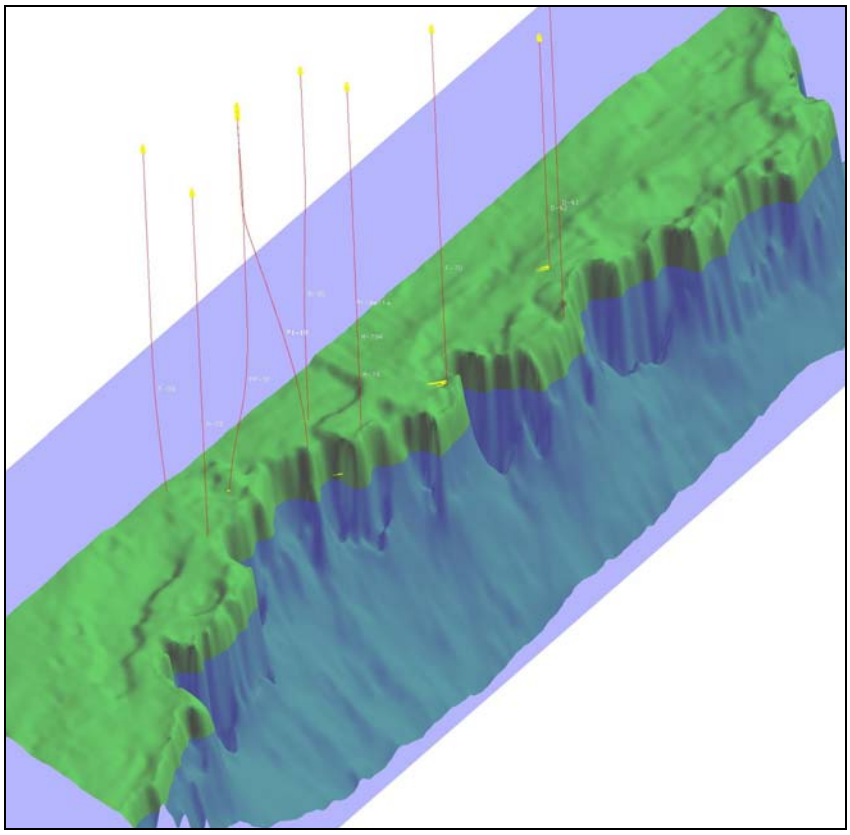

Figure 3: Abenaki 5 Surface, the 3-D block diagram shows the steep front of the Abenaki carbonate margin, the F-70 well is in the center of the image. Diagonal distance about 28 km.

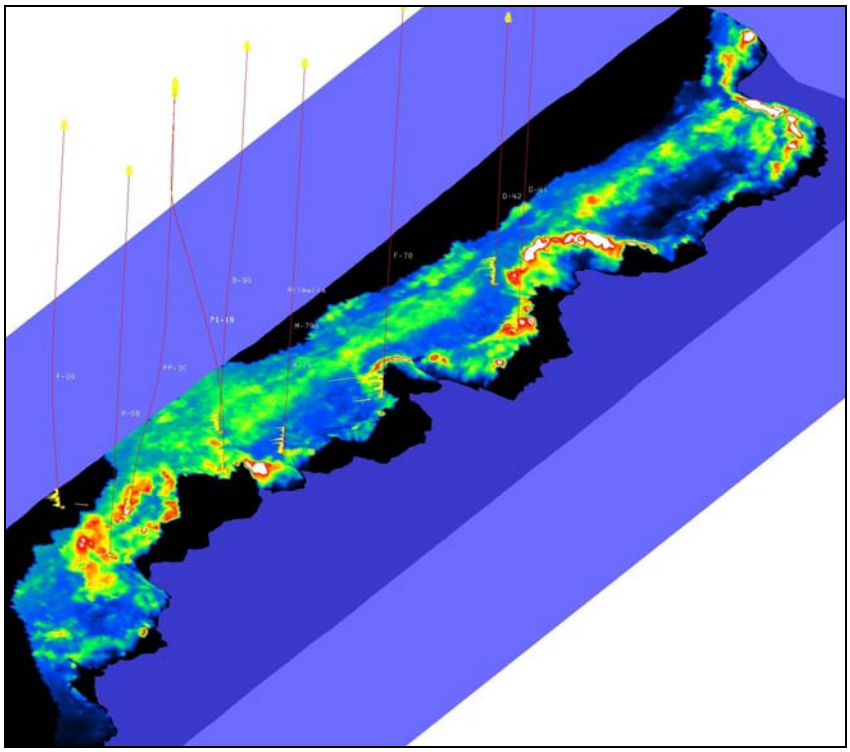

Figure 4: A phi-h map based upon a seismic porosity model, the hot colors represent areas of thick high porosity, the thick high phi-h zones along the margin edge are dolomitized and fractured, the thick zones behind the margin edge are the vuggy limestones of the platform interior; the F-70 well is in the center of the image. Diagonal distance about 25 km.

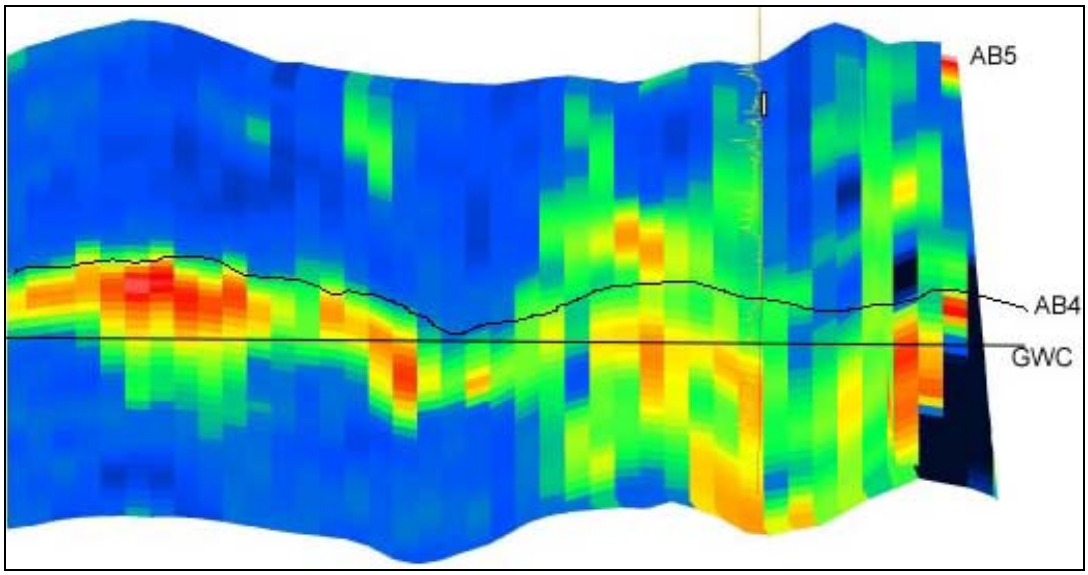

Figure 5: Seismic porosity volume through the F-70 well in the Abenaki 5 and 4, hot colors equal higher porosity, the core was collected from the top of the porosity zone at the blue to green transition.

Whole core recovery from the high porosity portions of the reservoir is poor due to jamming and failure to catch the rubbly, vuggy rock. Lost circulation had been encountered in several wells which precluded coring operations because of safety concerns. Nevertheless, limestone and some dolomite core in the reservoir had been recovered from the H-08 and PI-1A wells (see Appendix). In addition core had been recovered from early exploratory wells, L-97, and G-32, see Eliuk 1978 for detailed descriptions of the latter. A program of sidewall coring and FMI imaging of the reservoir were part of the routine petrophysical program to obtain fracture and lithology data even when full cores were not obtained.

Fracturing had been noted in some of the core and on associated FMI images. The rock recovered in the H-08 core is brecciated to some degree as well as fractured, probably caused by partial solution collapse of the high porosity zone in addition to wrench faulting (see Appendix). H-08 and PP-3C occur over linear features back of the margin edge which are believed to be wrench faults.

Well test analysis indicated dual porosity behaviour could explain some of the well flow behaviour observed. One possible model proposed was that a high permeability fairway was present at the carbonate margin edge. In 2003, when two new wells were planned to extend the field to the NE, it was decided to acquire additional core data. The F-70 well was drilled without problems and 24 meters of dolomite and limestone core was recovered from the upper part of the Abenaki 5 reservoir. This was achieved by good planning: aluminium sleeves, a controlled coring program, and good luck - a slightly tighter then average section so rubble was not encountered. In addition, a FMI image, Stoneley waveform analysis, and a PLT spinner survey were acquired at the well. The second well, D-41, did not have the same luck. The coring program was cancelled when partial loss of circulation occurred at the top of the reservoir. Sidewall cores, FMI images, and Stoneley wave data were collected from the D-41 well which supported the observations at F-70 that the dolomite was indeed fractured.

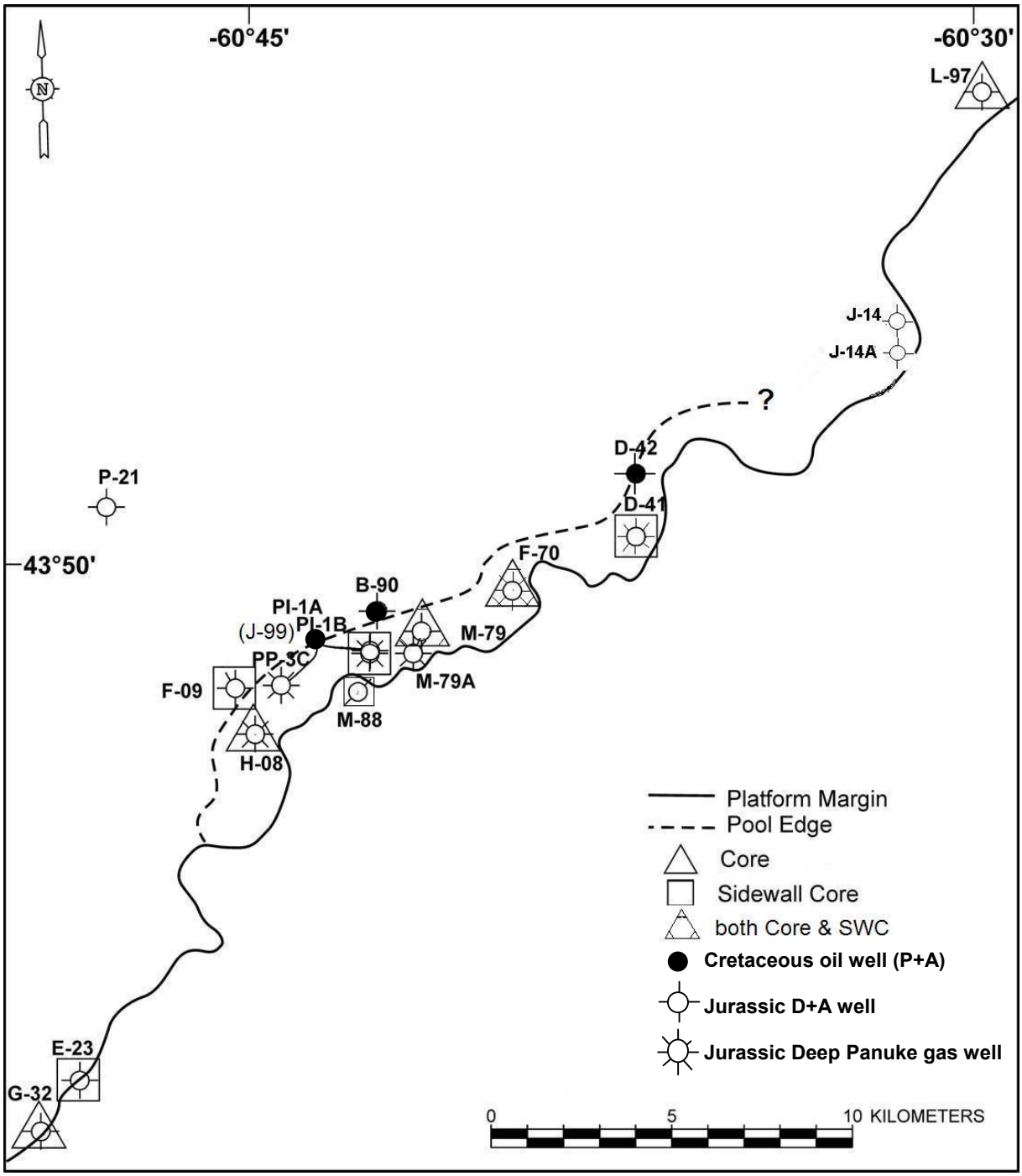

Figure 6: Well locations, type of core collected, the key core discussed in this presentation is from the Abenaki 5 cycle in the F-70 well. (modified with addition of post 2005 wells Dominion J-14 and J-14A). Comments on Deep Panuke area wells follows. The initial Deep Panuke discovery well PP-3C and PI-1A and PI-1B were drilled from the production platform at J-99 through former Cretaceous oil producer (PP) or injector (PI) slots and are highly deviated in their upper well bore. Panuke M-79A and Dominion J-14A are deviated wells whip-stocked from the original holes. Cohasset D-42 (rig released 1973) Demascota G-32 (rig released 1974) are the first and second tests of the Abenaki carbonate margin. D-42 and Panuke B-90 discovered oil in the overlying Cretaceous sands. MarCoh D-41 successfully offset D-42 but Musquodoboit E-23 proved G-32 was below the pool gas-water contact. Both Panuke B-90 and F-09 are highly oolitic but essentially non-porous in the Abenaki and thus define a stratigraphic component to the Deep Panuke trapping. More information including dip seismic on all the wells shown is give in Kidston et al. (2005).

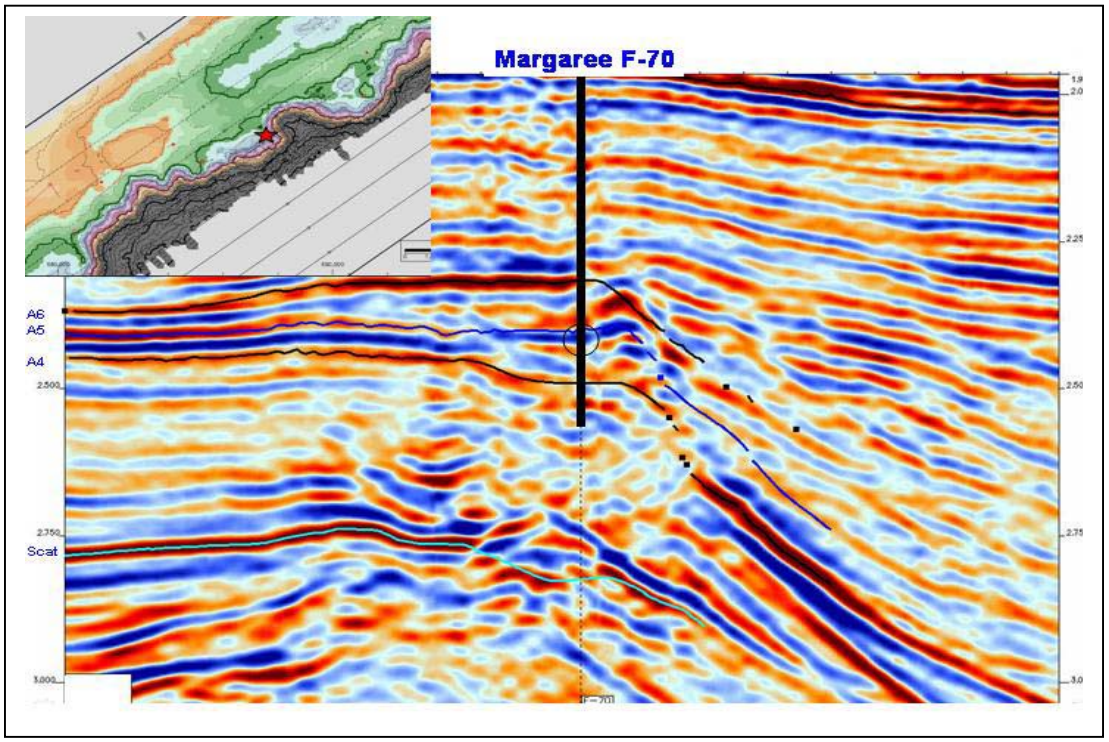

Figure 7: Seismic dip section through Margaree F-70 (from Kidston et al. 2005). Note inboard position relative to local small buildup

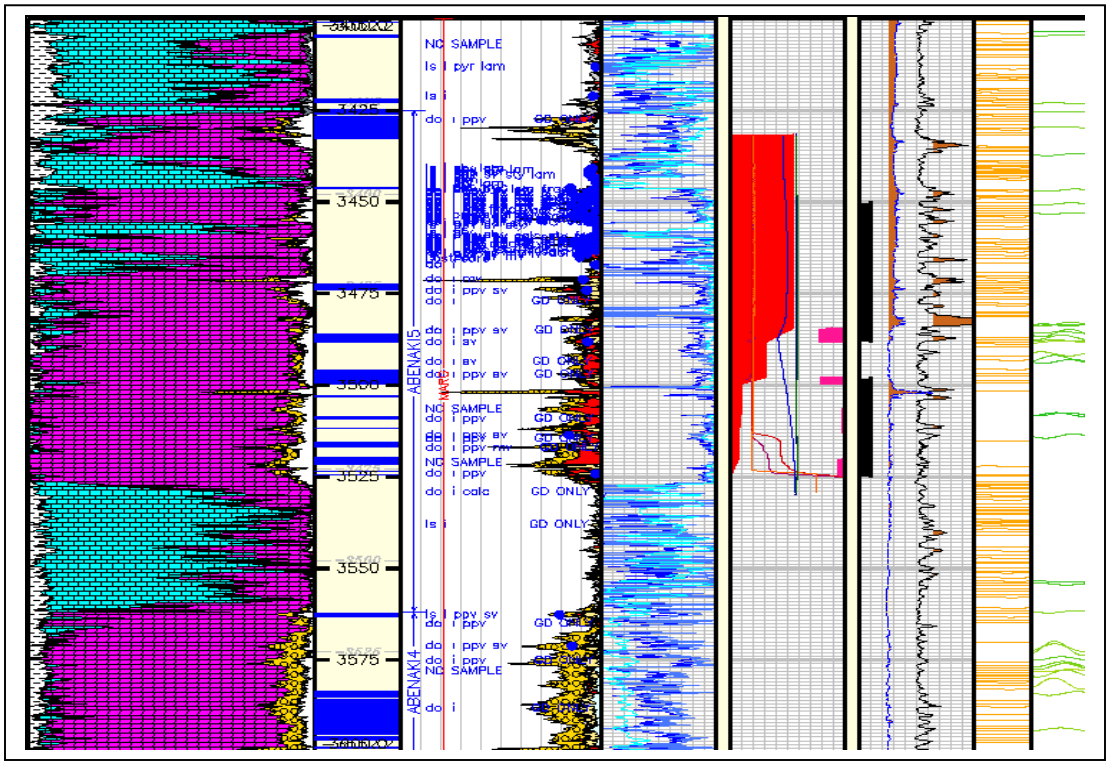

Figure 8: F-70 petrophysical interpretation and core location, from left, track 1, lithological interpretation; track two, blue indicates Stoneley wave attenuation (fractured intervals); track 3, porosity interpretation and core and sidewall core porosity, note the core is in the interval around 3450 m where all the blue core data annotation is clustered, other annotation is from sidewall cores; track 4, water saturation; track 5, PLT log interpretation, most gas flowed from areas indicated in pink (fracture swarm); track 6, calliper, density correction, perforations, track 7, bed boundaries picked from FMI; track 8, fracture events picked from FMI

Depositional Setting – Margaree F-70 core and well (L.Eliuk)

Set within a lithofacies transition of the F-70 well section from dominantly cleaner dolomite-rich carbonates up into slightly argillaceous limestone-rich carbonates, Margaree F-70 core #1 (3434-3458.7m) also captures a depositional facies transition in reef types and water depths (and/or nutrient-argillaceous content) that increase upward. Jurassic-earliest Cretaceous carbonates show three reef-reef mound type end members – coral (& coralline sponge), siliceous (lithistid) sponge and microbial crust (Leinfelder 1994, Leinfelder et al. 2002). From one of the first wells drilled on the Nova Scotia carbonate margin all three types are present and have been included in Abenaki facies association templates (Eliuk 1978, Eliuk and Levesque 1989, Wierzbicki et al. 2002). The associated depositional model is shown in Figure 9 (Wierzbicki et al. 2002). The relationship of the whole F-70 Abenaki section to the core is shown in Figure 10 and of

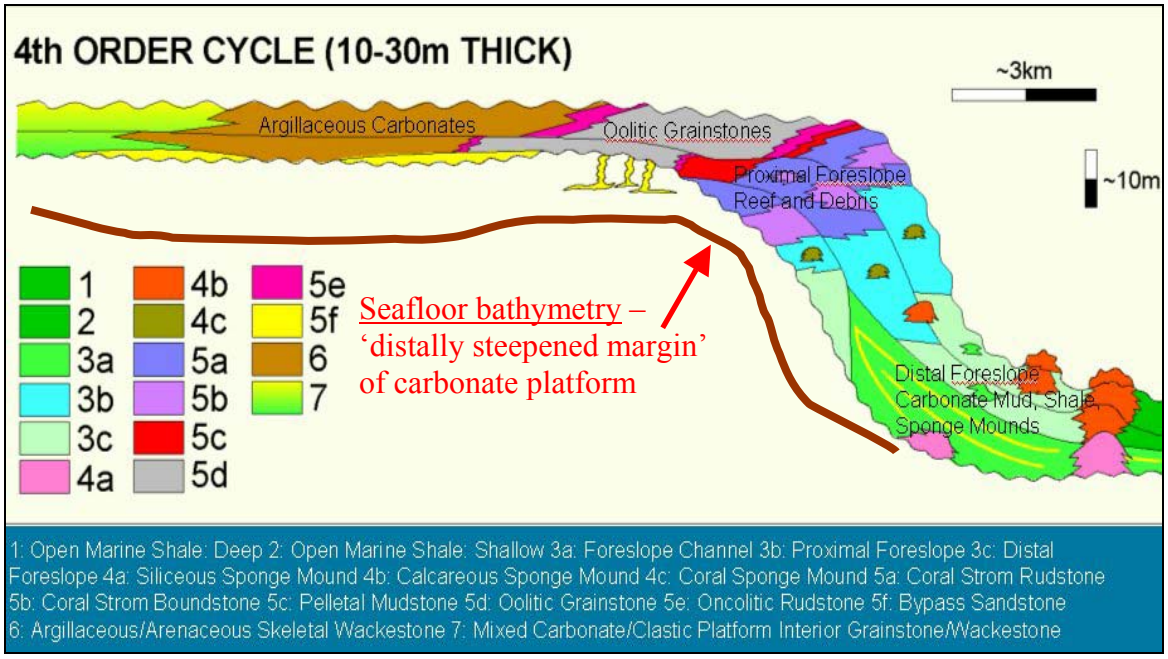

Figure 9: Abenaki facies model, modified from Wierzbicki et al, 2002.

core # 1 with its thin reef types named in Figure 11. They tell a story of what happens around an Abenaki reefal build-up from shallower to deeper water or from further to closer proximity to the major Sable Island paleodelta or both. Between interpreted forereef dolomitized and even inclined beds, the core has 4 reef examples transitional between the 3 end-member reef-reef mound types of the mid-Mesozoic. The facies model (Figure 9) shows a simplified continuous progression from the shallow oolites near the inner platform margin seaward through a reef-rich outer margin downdip into the forereef slope. The reality is more complex as seen on seismic (Figure 3 and 7) where there is a topographically irregular zone over a kilometre wide where various buildups occur and may even have local landward or westward forereef slopes. This is what Eliuk (2004 and in Figure 9) refers to as a distally steepened margin, all in variably deeper water than the inboard flexure, until the outboard flexure then more distal slope is reached. The margin is further complicated by likely early collapse of portions of the margin and later down to the basin and wrench faulting (Wierzbicki et al. 2002, 2006; Weissenberger et al. 2006)

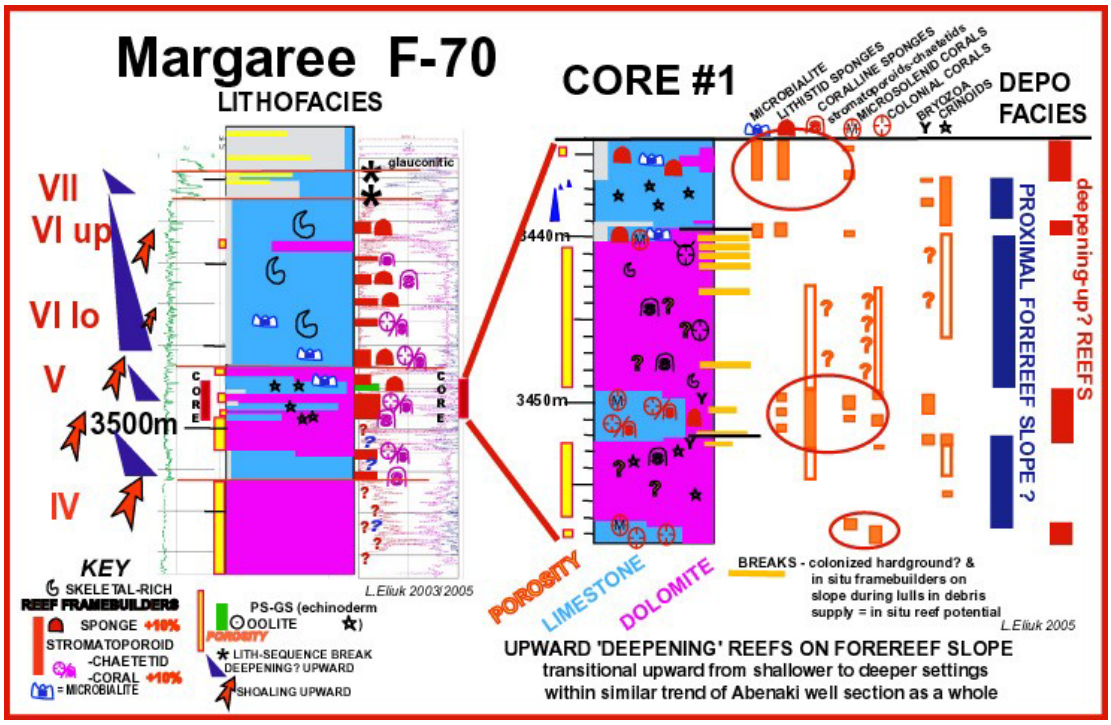

Figure 10: Abenaki lithofacies based upon core and ditch cutting interpretation by Eliuk, the Abenaki 4 is a shoaling up cycle, the Abenaki 5 starts with a marine incursions, shoals, then deepens, the Abenaki 6 attempts to shoal at it's base then drowns.

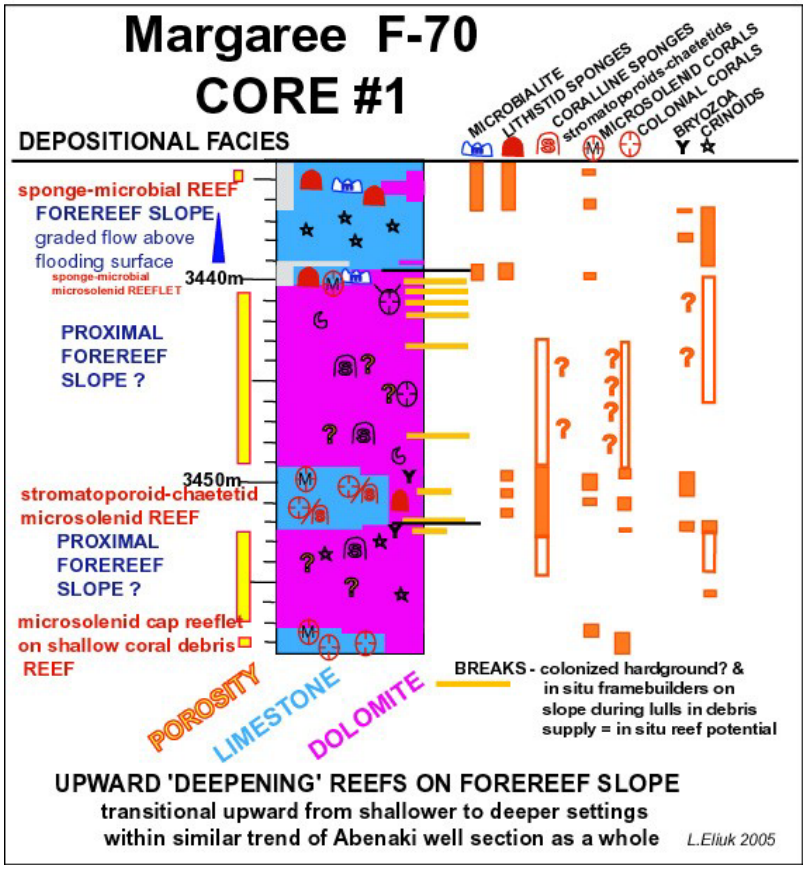

Figure 11: F-70, detailed Abenaki 5 core description, dolomite replaces foreslope reefal debris, boundstones undolomitized.

Based on F-70 cuttings analysis, the mainly argillaceous-carbonate mud-supported limestone of the upper Abenaki (sequences VII and VI) are interpreted to be dominantly forereef slope with periods of thin deeper-water reef colonization. Initially these reefs are a mix of corals, coralline sponges (stromatoporoids-chaetetids) and lithistid sponges with a microbial component. But upward there is a progressive decrease in corals (along with microbialite content?) then stromatoporoids leaving only the lithistid sponges. This change indicates increasing water depth and/or nutrient-argillaceous content upward. The lack of even derived oolites as parts of slope debris in the whole section supports the seismic geometries (Figure 7) showing that not only was F-70 drilled on the back or bankward-side of a partially collapsed margin-edge build-up but that it penetrated material shed and growing in deeper water on the southwest side of a local pinnacle or raised rim. Downward (sequence V) there is a decrease in sponge and microbial content and an increase in dolomite to 100% in the bottom 100 metres (sequence IV). The presence of abundant crinoids at the top of sequence V indicates slope deposition continued but interbedded with increasing amounts of coral and stromatoporoid reef or reef-derived sediment downward. Thus the dolomitized sections, whose depositional facies is problematic even with the help of sidewall cores, are inferred to be reefal or at least shallow-water carbonate bank.

Core #1 is well placed to show the litho- and depo-facies transition. The limestone intervals are reefal except for 3 metres of well-cemented normal-graded crinoid-rich slope debris beds (channel with possible submarine cement) near the core top. The thick dolomite intervals are interpreted to be proximal forereef slopes with debris from a shallower-water coral-stromatoporoid reef intermixed with minor slope material such as crinoids and bryozoa. An originally porous finer sand matrix may have localized the dolomitization. During breaks in slope sediment supply, hardgrounds (?) and framebuilder colonization occurred. If the breaks were long enough a deeper-water reef built up. Analysis of percentage framebuilder contribution shows a progressive change that is interpreted to result from progressively deeper (or/and more nutrient-rich and argillaceous content which due to increased turbidity has the effect of increased depth if the organisms can handle the greater clays-nutrients). The basal few metres of the core has 16% microsolenid hexacorals and 28% other colonial hexacorals in a rudstone indicating shallow-water reef-derived or even storm-affected in-situ reef. These rubbly beds are capped by a 0.5 m in-situ pure microsolenid coral reeflet. The next limestone reef interval, above a thin crinoid–rich possibly transgressive lag limestone, has less hexacorals (15%) and microsolenids (8%) but more stromatoporoids-chaetetids (21% collectively coralline sponges) and lithistid sponges (14%). Capping the thick foreslope dolomite bed with its increasing number of sedimentation breaks is a microbial-sponge–microsolenid coral reeflet (0.5m thick and 12%, 15% and 11% respectively). Of the colonial hexacorals, microsolenids range into deeper and more turbid waters. At the top of the core a microbialite-lithistid sponge reef with some scattered microsolenids (16%, 21% and 9% respectively) form complex consortia with early-cemented high depositional angles (and possibly structural dip due to later rotation of whole section). Some solitary corals are present. Locally there are crusts of lithistid sponges overgrown by sponge-microbialites capped by bioeroded tabular microsolenid corals. Taken as a whole these changes indicated progressively deeper (more nutrient-rich?) water upward over the cored interval. The presence of periods of reefing on the slope indicate that the forereef slope is not just a sediment sink but supplies significant amounts of its own sediment.

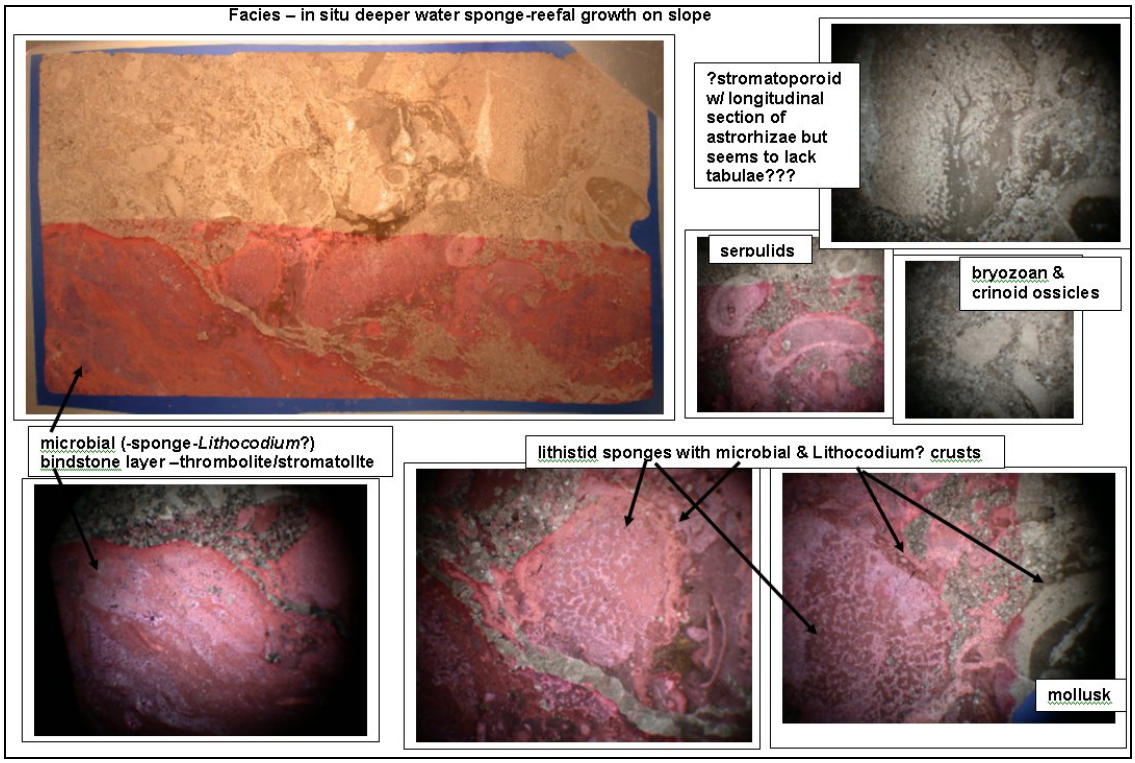

Figure 12: Thin section photographs from a deeper water sponge reefal facies, F-70 core 1, 3438.6 m.

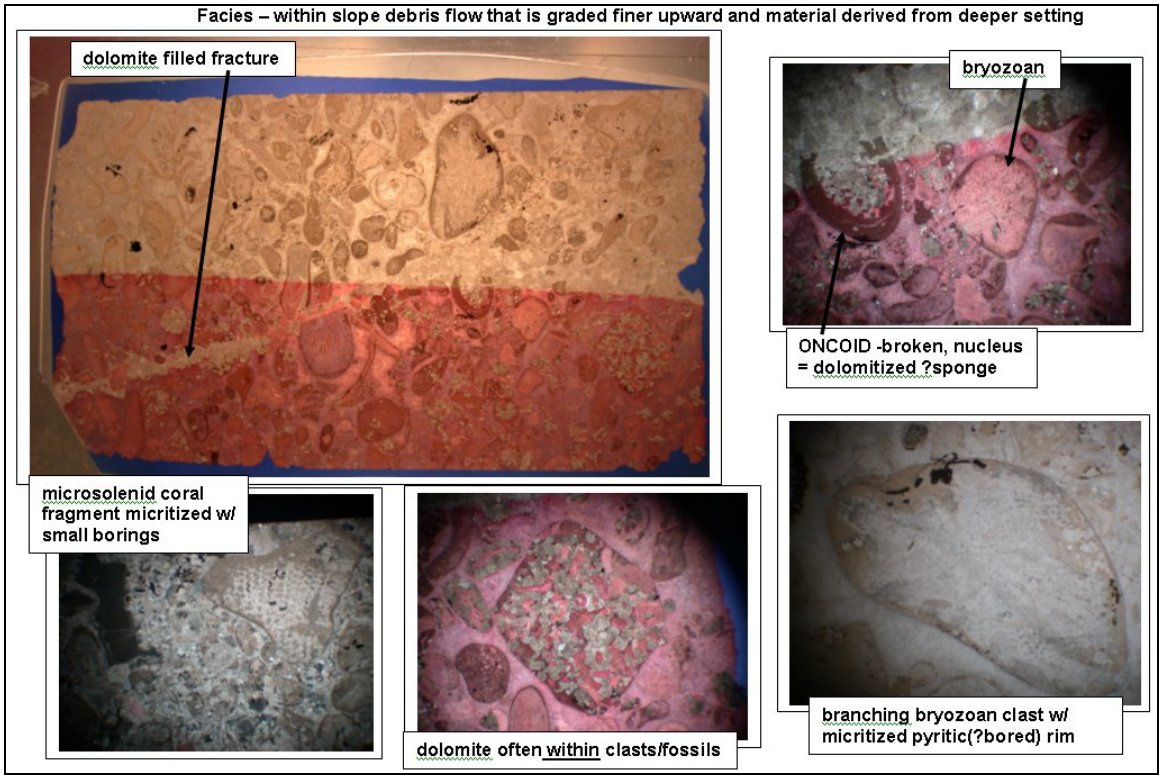

Figure 13: Facies: slope debris flow, fining upward dolomitic limestone, crinoid bryozoan grainstone with scattered reefal debris, F-70 core 1, thin section at 3437.55m with details enlarged.

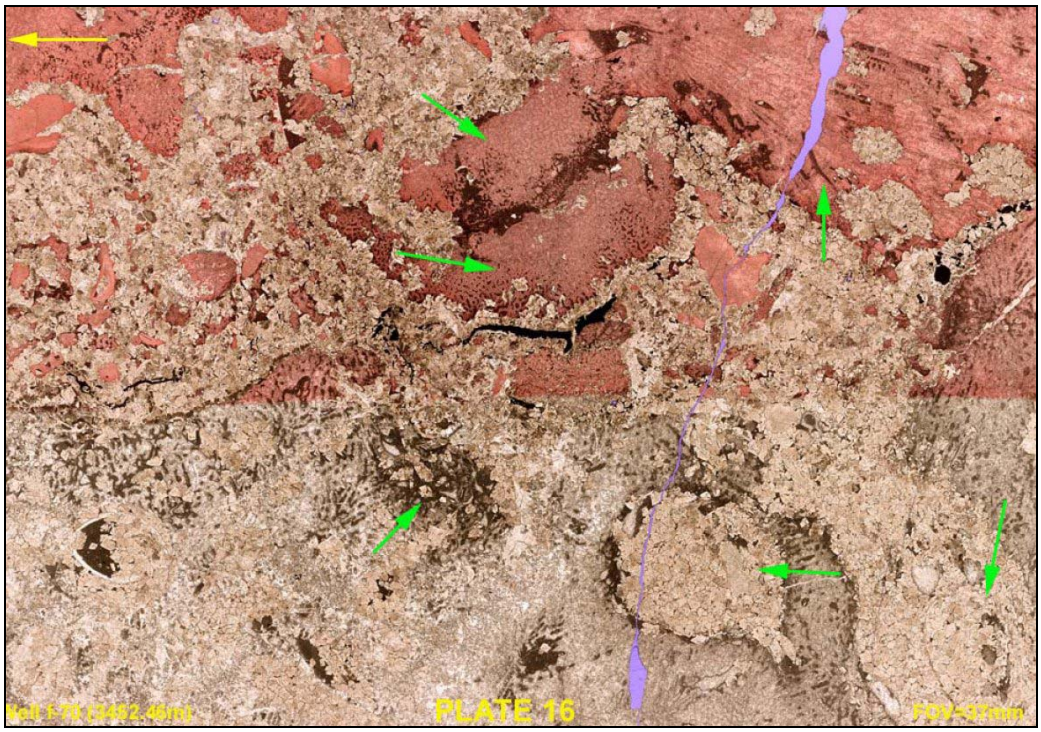

Figure 14: Facies: upper foreslope skeletal packstone, coral, stromatoporoid, sponge debris, dolomite replacing matrix and partially replacing fauna, thin section field of view 3.7 cm, F-70 core 1, 3452.45m.

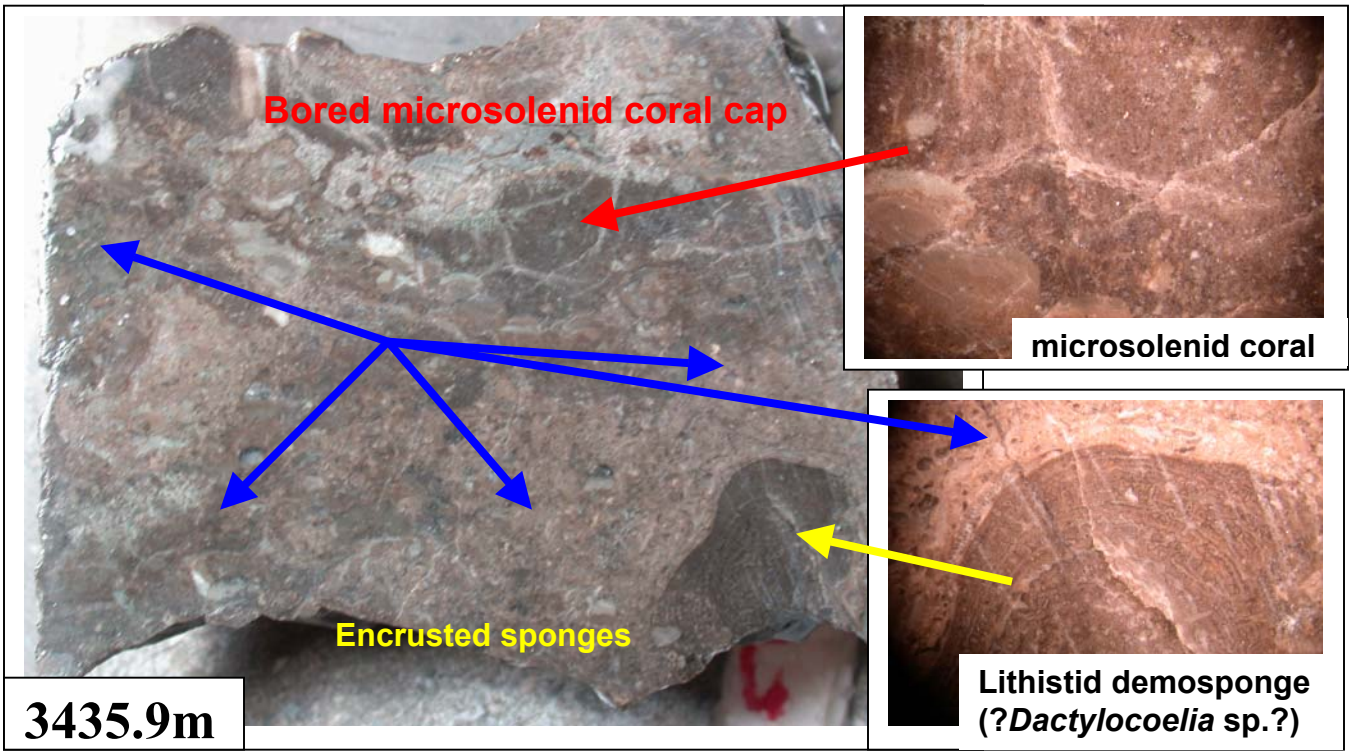

Figure 15: In situ reeflet-crust succession that occurs at a number of levels where lithistid demosponges are overgrown by microbial (and sponge) crusts and these often are capped by bioeroded microsolenid corals (a deeper water colonial hexacoral). These thin reefal buildups typically are not dolomitized and perhaps their early cementation made them less permeable to dolomitizing fluids as compared to the thicker grainier dolomitized foreslope interbeds. In places both the sponges and microsolenid corals have platy vase-like forms further indicating their deeper-water low-energy setting.

Figure 16: Core slabs, each slab 8.5 cm wide, dolomitic limestone, stromatoporoid-cabbage head coral rudstone in a skeletal packstone matrix, F-70 core 1, 3457 to 3458.7m (top left to bottom right). Note overturned coral head at base of core. Interpreted as shallowest water coral debris reef subject to storms or derived from such a reef and re-deposited on reef flat or proximal forereef slope.

Diagenesis (Jeff Dravis)

Seventeen thin sections were cut from the various facies and lithologies present within the core and examined by Jeff Dravis using enhanced light techniques (Dravis et al 1985). Samples examined petrographically from Well F-70 were dominated by dolostones and dolomitic limestones. This well appears to contain more dolostones than other Panuke wells drilled to date. Better preserved porosity, although generally not high, was associated with dolostones and was created during deeper-burial diagenesis. Dolomites replacing host Abenaki limestones were emplaced during burial, given their relationship to pressure solution fabrics (Dravis 1992). Preserved porosity generally was low, consisting of secondary intercrystalline (in pods of dolomites) and vuggy porosity. Several Abenaki dolostones exhibited relict depositional grains and at least a packstone texture when viewed with enhanced petrographic techniques, see Figure 17.

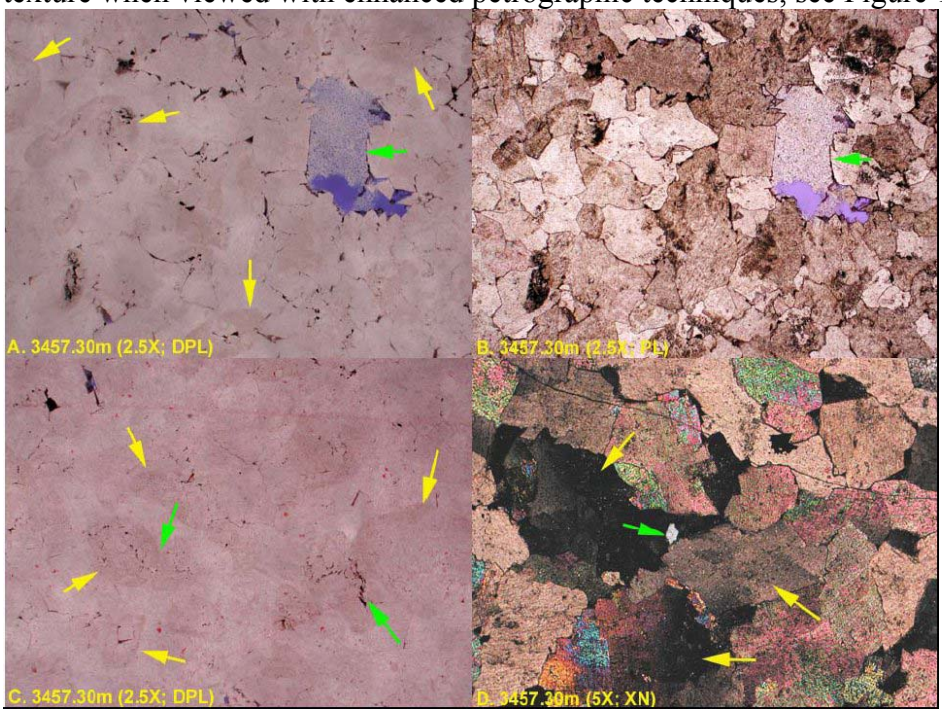

Figure 17: Thin section microphotographs: a) field of view (fov) 5.5 mm, enhanced light reveals dolomitized peloids and a dolopackstone texture, pore infilled with kaolinite (green arrow) requires acidic fluids for precipitation; b) fov 5.5 mm, standard petrographic light, textures not visible; c) fov 5.5 mm, enhanced light shows grains embayed and sutured, indicates a lack of precompaction cement, implies replacive dolomites deeper burial; d) fov 3 mm, crossed nicols reveal slightly to strongly undulose extinctions of replacive dolomite crystals, these saddle like effects are invariably associated with dolomites emplaced at depth under higher temperatures.

Preserved porosity, typically low to moderate in abundance, was secondary vuggy and moldic, the later related to partial dissolution of relict grains or dolomite crystals. Many dolostone samples contained noticeable amounts of macrocalcites, many of which were strongly twinned. Evidence for deeper-burial secondary porosity development in these dolostones included preservation of secondary porosity along pressure solution seams, secondary vuggy porosity cutting such seams, partial dissolution of relict grains already sutured by pressure solution, dissolution of burial replacive dolomites and dolomite cements, including saddle dolomites, and burial fractures terminating into secondary porosity.

The presence of authigenic quartz and kaolinite cements implied passage of acidic pore fluids that could explain observed secondary porosity development. Emplacement of late-stage calcites, precipitated from warmer (hot?) burial fluids, also could explain observed dolostone dissolution. Such relationships were observed in Abenaki samples from other Panuke wells nearby.
The diagenetic events observed, supported by fluid inclusion and isotopic analysis supported the earlier conclusions of a muddy reef being altered by early burial and cementation and subsequently having porosity enhanced by dolomitization and dissolution (Dravis 1999, 2001; Wierzbicki et al 2002; Eliuk 2004; and Wierzbicki et al 2006).

Core Fracture Analysis Methodology and Observations (K.Gillen)

Core from Margaree F-70 was reassembled into continuous segments. Fracture data obtained from these segments were restored to in situ orientation by matching bedding, stylolites and argillaceous layers measured in core to those seen in the image log.
Figure 18 shows a roseplot of the in situ strike of all fractures in core which could potentially inhibit flow (i.e. filled fractures in the case of this core). Three populations are identified. The strike orientations of the three groups are: NW-SE (dominant), NNE-SSW and NE-SW.

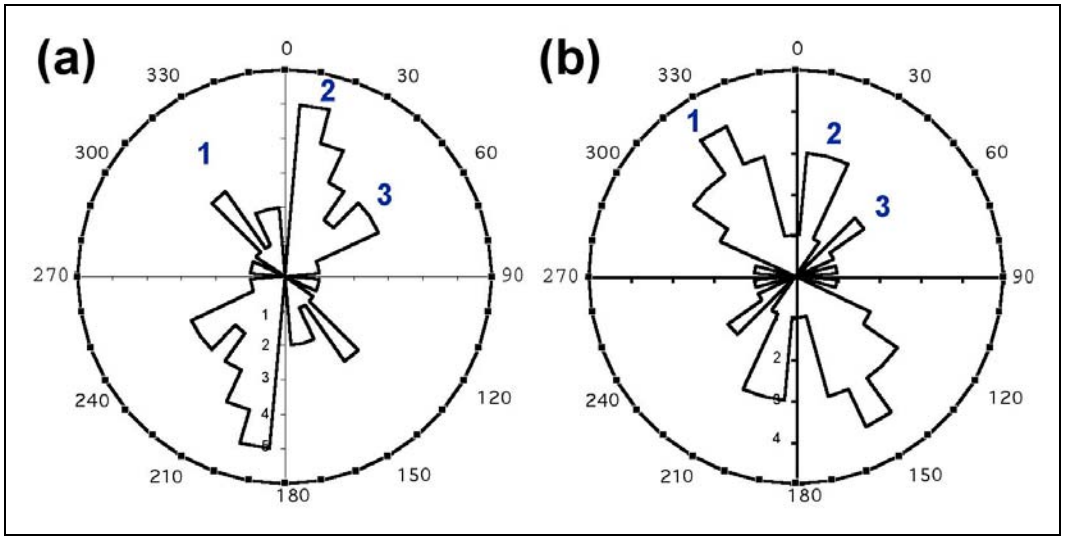

Figure 18: Roseplots of fracture orientation

A roseplot of the strike of all natural fractures which could potentially contribute to flow is illustrated in Figure 18. The strike distribution of these show similar trends to those of the filled fractures, and suggest that the populations identified previously (populations 1, 2 and 3) might be present in these data. However, the relative proportions of each population are different. Table 1 lists their relative proportions and compares them to the filled fracture data.

POP #	STRIKE	FILLED FRACTURES	FRACTURES WHICH COULD POTENTIALLY CONTRIBUTE TO FLOW
1	NW-SE	dominant	subordinate
2	NNE-SSW	intermediate	dominant
3	NE-SW	subordinate	subordinate

Table 1: Relative proportions of each population.

Similar strike trends are apparent in the conductive fractures seen in the image log over the cored interval, but poorly defined due to the low number of data points.

FRACTURE ANALYSIS CONCLUSIONS

1. Although other minor directions are represented, the dominant orientations of natural fractures which potentially contribute to flow fall into three groups with the following strike values: NW-SE, NNE-SSW (dominant) and NE-SW.
2. The dominant orientations of natural fractures which potentially impede flow fall into three groups with the following strike values: NW-SE (dominant), NNE-SSW and NE-SW.
3. Similar strike trends are apparent in the conductive fractures seen in the image log over the cored interval, but are poorly defined due to the low number of data points from the image log.
4. Filled fractures appear to be approximately perpendicular to bedding.
5. Fractures appear to be open (or have been open at one time) due to such mechanisms as dissolution, and processes related to stylolite development. Other mechanisms may contribute.
6. Only 2% of the natural fractures observed in core cut completely through the core, suggesting that the average fracture size is quite small. Fracture height appears to be limited by bedding and stylolite surfaces in many cases.
7. The average direction of the minimum in situ horizontal stress is 081.4^{o}. This estimate is based on only a few coring-induced fractures, and has a low degree of confidence.
8. Some breaks in the core from Margaree F-70 display a character which suggests the presence of microfracturing. The in situ orientation of this fabric is 164^{o}, but is based on only one data point and thus has a low confidence.
9. The match between fractures observed in core and those seen in the image log is poor. This is probably due to the small size of the natural fractures in this interval. Some could be too short to be seen in the log, while others might not make it across the gap between the core and the borehole wall.

Discrete Fracture Network Modeling Methodology and Observations (R. Ackermann)

The primary goals of the modeling were to 1. evaluate extant fracture data from borehole image logs (BHI) and core studies; 2. define fracture sets based on orientation, structural

context, and facies relationships; and 3. generate effective fracture permeabilities and porosities for use in dynamic reservoir simulation.
The work program for this effort was split into 5 phases:

1. Data collection & review: construction of the 3D model based on a geo-cellular model (built in gOcad) provided by EnCana; review of extant fracture interpretations/studies; formatting and integration of well (static & dynamic) data into the 3D model; formatting and integration of maps (seismic attributes, other) into the 3D model.
2. Fracture set definition: splitting of observed fractures into orientation sets based on facies associations, structural position, and interpreted dynamic behaviour.
3. Fracture local permeability modeling: construction of discrete fracture network model using results of phase 2 (above), and other available input controls from phases 1 & 2 (above).
4. Dynamic modeling: calibration of the fracture network model using available PLT and well test data.
5. Equivalent parameters export and reporting: Export of full-field equivalent fracture permeability, porosity, and equivalent matrix block dimensions for use in dual-media reservoir simulation; report summarizing workflow, computations, interpretation of results, and uncertainties.

The primary tool for the fracture analysis and modeling was FRACA, a discrete fracture network (DFN) modeling package, where each fracture and subseismic fault is modeled as an individual hydraulic object. The DFN is discretized into a 3D resister network and a pressure boundary condition is applied in order to calculate an effective fracture permeability tensor, equivalent matrix block dimensions, and fracture porosity information for each cell in a reservoir model. This information is designed to be used in dual-media dynamic simulation. FRACA permits calibration of the fracture network to field dynamic data by providing a flow solver to generate PLT and well tests from the modeled network.

Fractures at Deep Panuke were divided into two sets, a dolomitized margin edge (HPRF) and a dominantly limestone mid-reef (MRF). HPRF wells contain fractures whose orientations span the compass leading to good connectivity; these are caused by regional stress and deformation along the margin edge. MRF wells contain fractures that strike dominantly NE and dip NW and are more widely spaced, resulting in a much lower connectivity then in the HPRF, see table 2.

	Low Por. Lst.	High Por. Lst.	Low Por. Dol.	High Por. Dol.
Bed Thickness (m)	0.49	0.88	0.8	1.22
HPRF Frac Spacing	2.22	6.36	0.41	2.17
MRF Frac Spacing	19	5.57		8.52

Table 2: Fracture Modeling Data, limestone generally has a wider fracture spacing then dolomite, rock in the HPRF has a tighter fracture spacing then rock in the MRF.

Uncertainties in fracture length and hydraulic conductivity were assessed and several models created and refined via iterative well test matching. The resulting best models were reviewed and were tested against the only well with PLT data, the F-70 well. Below is an example of one such test. An essential problem that cannot be resolved is that a

fracture may be open at the well bore, but may in fact be isolated and hence will model as if connected unless it is removed. A similar challenge arises if a given fracture is clogged with drilling fluids. As it is impossible to determine from the well bore if the fractures are connected, the only way to get a perfect match would be to have an iterative loop of removing fractures until the match was good. Another uncertainty is the contribution of matrix zones of high porosity or permeability that exist in the well, but have been lost in the fine-scale modeling process. One such zone may exist at a depth of 3522 m. If the modeled PLT were allowed to "kick" at that depth, the match would be nearly spot-on. Rather than spending time tweaking a single well's response at this stage of the flow characterization, the goal is to produce a qualitative match such that the cumulative modeled production profile has the same general character as that of the observed production profile.

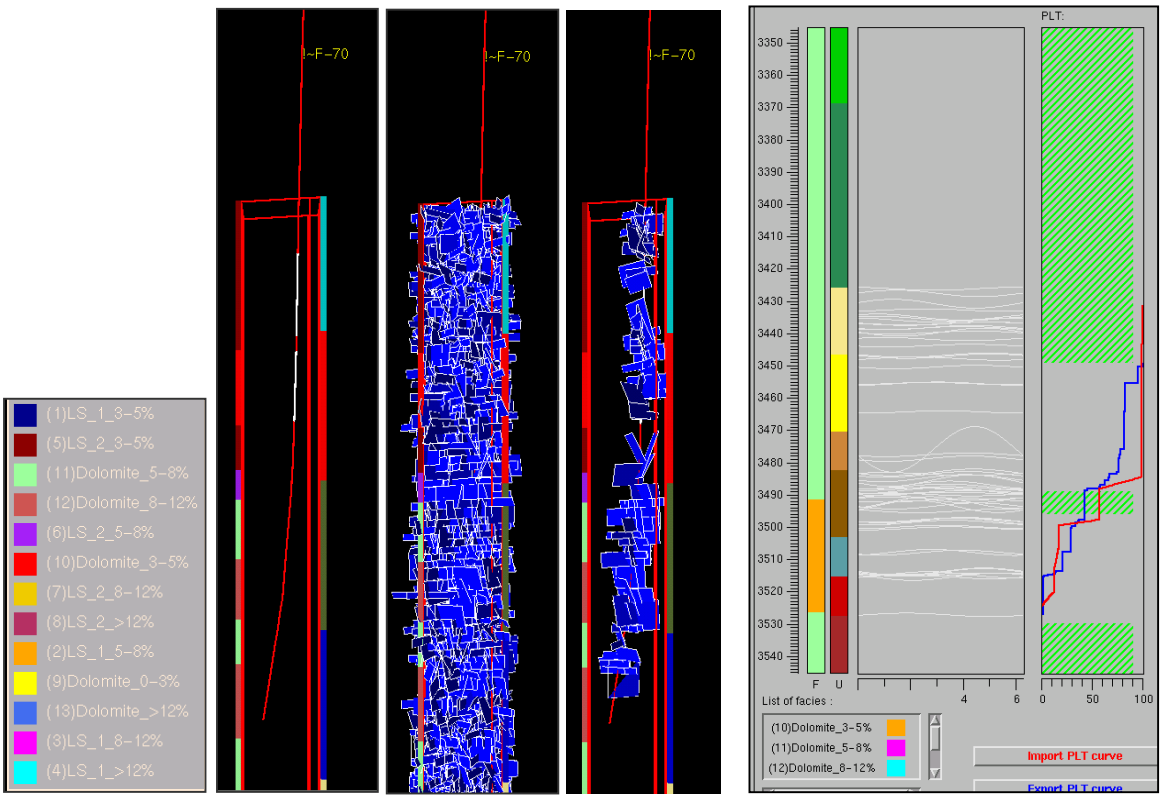

Figure 19: Views of the PLT simulation in FRACA for well F-70, from internal report by Beicip Inc. for EnCana. The three 3D images in the middle of the figure show the well bore with perforations in white, facies intersected by the well shown along the left side of the box, and reservoir units on the right. The middle 3D view shows all fractures modeled around the well, and the right 3D view shows only those fractures connected directly to the well bore (fractures connected to those fractures are not shown). This model is conditional, meaning that the fractures modeled at the well bore honor those observed in the BHI data. The panel on the right is a well bore view with MD, facies, and reservoir units displayed with fracture-well bore intersections as white sinusoidal traces. To the right are the perforation intervals and cumulative flow, the modeled PLT is shown in blue, the PLT observed in the well is shown in red.

Discussion: F-70 Core Interpretation

Facies and Diagenesis

The existing facies model developed in 2002 was appropriate to describe the facies observed in the core. The Abenaki carbonate platform at Deep Panuke was deposited in a distally steepening ramp geometry with shallow water reefs forming basinward of oolitic grainstone shoals. Basinward of the reefs are debris flows of coarser reefal material and deeper water muddy carbonates as well as sponge bioherms. During relative rise in sea level these deeper water sponges and microbolites can encrust the flanks and tops of the shallow water reefs. The key factor for diagenesis is that the reefs, both shallow and deep, tend to be lower energy and have a muddy matrix.

During burial, diagenetic fluids preferentially altered the muds and associated allochems creating vugs from the fossils and recrystallizing the mud to dolomite or earthy limestone porosity. In contrast the high energy oolitic grainstones shoals were predominantly cemented tight shortly after burial and were not significantly altered when the hydrothermal fluids accessed the system.

Fracturing

The early fracture analysis was carried out on limestone core and FMI images and few fractures were observed. This was likely due to limestone being more ductile then dolomite and the wells being some distance back from the margin edge. In addition observed fractures were short, as they tended to terminate when they encountered a vug or a change in fabric like a coral head. The F-70 and D-41 wells encountered much more dolomite in the Abenaki 5; these wells are more fractured, especially in the non-vuggy dolomites. Analysis of the dolomites have led to the conclusion that not only is the dolomite fracture spacing much closer then in the limestone but the fracture orientations are more random which leads to much better connectivity between fractures.

As part of a borehole stability study the present day stress field was examined. Deep Panuke occurs at a point where the stress field changes direction from minimum stress of NW-SE to E-W. This is sub-parallel to the crest of the plunging anticline that the Panuke pool is draped over, while the regional minimum stress is perpendicular to the platform edge. It appears that deep seating structural features are influencing the present day stress field.

Paleo stress orientation is revealed by the orientation of the fractures that are observed on the M-79, F-09, and H-08 FMI and RAB images. Fracture swarms in the F-09 well bore generally dip to the NW and SE at 70 to 90 degree angles hence minimum stress would have been roughly perpendicular to the basin edge, similar to the present day regional system. Fractures in the M-79 well bore are more randomly oriented but also are dominated by NW and SE dipping fractures. Minimum stress would have been perpendicular to the margin as well. Timing of fracturing relative to dolomitization and leaching is ambiguous. The fractures in the limestone in H-08 appear to have been leached open and were in place prior to leaching. Fractures in F-70 were obviously post dolomitization but do have indications of enlargement by leaching and saddle dolomite cements present. This suggests that burial dolomites were in place and fractured and then additional hydrothermal fluids moved through the fracture system.

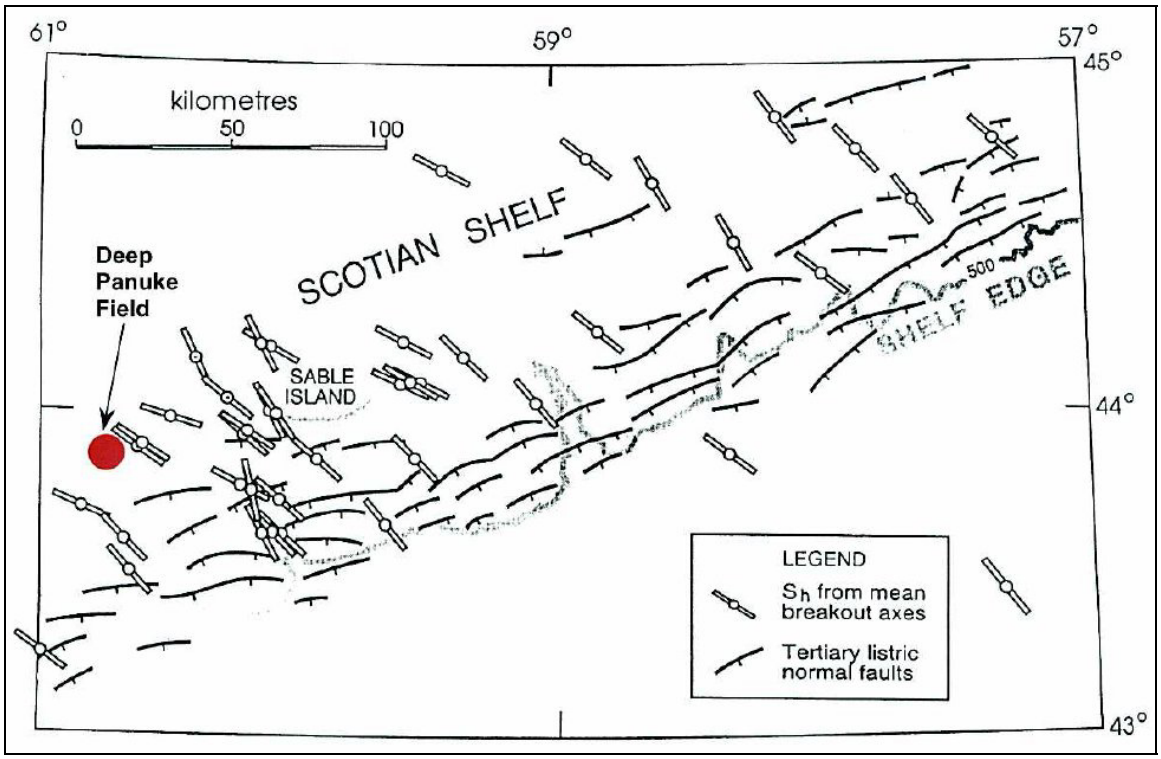

Figure 20: Present day stress from borehole break-out, shown is minimum stress direction, from Yassir and Bell, 1994, modified by Advanced Geotechnology Inc.

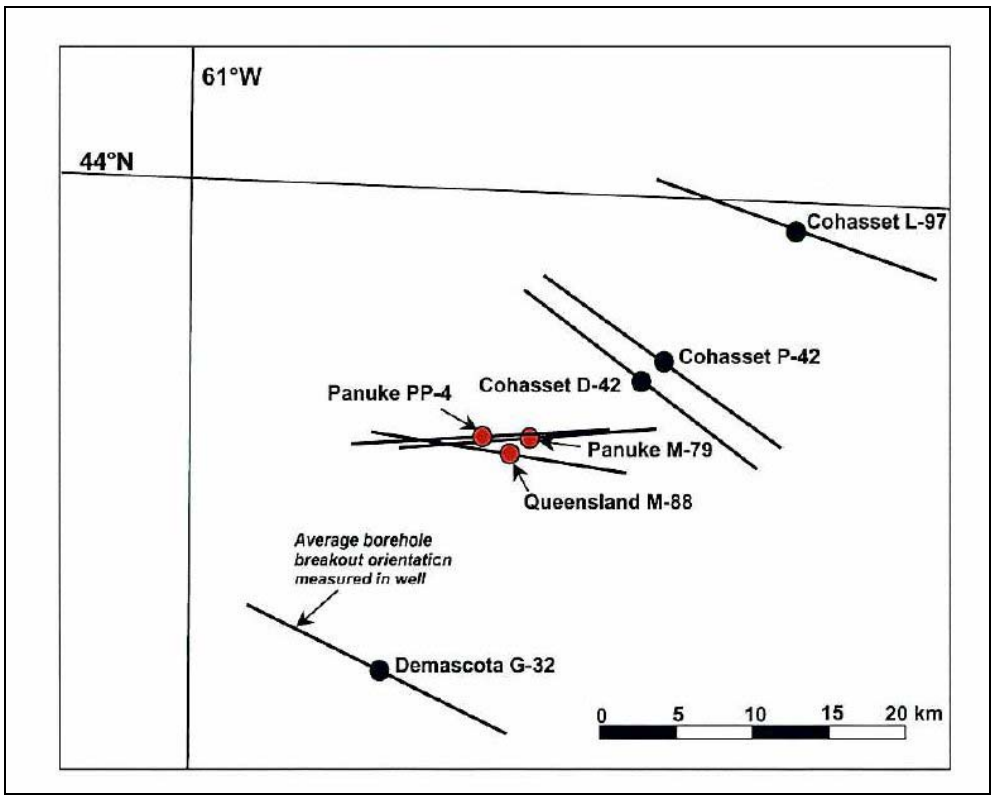

Figure 21: Present day borehole break out orientation, same as minimum stress direction, from Advanced Geotechnology Inc., dominant minimum stress is perpendicular to the Abenaki carbonate margin edge but does rotate by about 45 degrees to be perpendicular to local scallops in the carbonate margin and/or sub-parallel to the axis of an underlying anticline.

The Production Log Test (see Figure 19) indicates one of the fractured intervals appears to have exceptional permeability and dominated flow during the well test of F-70. The PLT result shows the limitations of well bore images and near well bore petrophysical techniques such as Stoneley wave analysis. A highly productive fracture set is obviously well connected at a larger scale but looks the same as low productivity isolated open fractures at the well.

The discrete fracture network modeling technique created models with a thick dolomitized and fractured margin parallel flow unit and much less fracturing in limestone towards the platform interior. The short length and variable orientations of the fractures resulted in good lateral connectivity and fair vertical connectivity in the dolomites. The results match that used in simulation models of the reservoir and provide a good fit to well tests. Current simulation modeling of the reservoir is being done using a dual porosity model.

The F-70 core was the key element to understanding the nature of fracturing in the reservoir. Prior to the core being obtained well test data indicated that fracturing may be present but the well behavior could be explained by heterogeneous touching vug porosity systems as well.

Acknowledgements: We would like to thank John Hogg and Tom Craig of EnCana, and EnCana for permission to present this material. Jeff Dravis and Ihsan Al-Aasm for undertaking the diagenetic studies which illuminated the diagenetic history of the reservoir. Derry Eddy, Tarun Kashib, and Blaine Hujber for the well test matching and simulation modeling which was used to constrain the fracture model. HEF Petrophysical for their FMI interpretations and Advanced Geotechnology for their stress field interpretation. Lastly, thank you to the East Coast Exploration team that discovered the reservoir, John Hogg, John Weissenberger, and Ian Delong. Leslie Eliuk thanks my co-authors and EnCana for allowing me to present this on their behalf in 2008. Contact Eliuk by email at geotours@eastlink.ca.

References

Dravis, J.J. 1991. Carbonate petrography - update on new techniques and applications, Journal Sedimentary Petrology, v. 61, p. p. 626-628.

Dravis, J.J. 1992. Burial dissolution in limestones and dolomites - criteria for recognition and discussion of controls: a case study approach (Pt. 1: Upper Jurassic Haynesville limestones, east Texas; Pt 2.: Devonian Upper Elk Point dolomites, western Canada, AAPG/CSPG Short Course "Subsurface Dissolution Porosity in Carbonates," Calgary, Canada 171 p.

Dravis, J.J. 1999. Petrographic evaluation of samples from the Abenaki Formation, offshore Nova Scotia (wells G-32, L-97, P-23, G-13, P-15, I-100, K-62 and PP3C), Confidential technical report for PanCanadian, 11 p.

Dravis, J.J. 2001. Diagenesis and porosity evolution of Abenaki carbonates, Panuke Field, offshore Nova Scotia, implications for controls on reservoir quality, Confidential technical report for PanCanadian, 48 p.

Dravis, J.J. and Yurewicz, D.A. 1985. Enhanced carbonate petrography using fluorescence microscopy, Journal Sedimentary Petrology, v. 55, p. 795-804.

Eliuk, L.S. 1978. Abenaki Formation, Nova Scotia shelf, Canada – depositional and diagenetic model for a Mesozoic carbonate platform. Bulletin of Canadian Petroleum Geology, v. 26, p.424-514.

Eliuk, L.S. 2004. History of the practical application of a failed? dolomite model (mixing zone) to the "Demascota Dolomite Beds" of the Abenaki Formation, Nova Scotia Offshore Late Jurassic paleocontinental shelf carbonate margin; *In:* J . Packard, and G. Davies (Eds.), Dolomites , The Spectrum: Mechanisms, Models, Reservoir Development; Canadian Society of Petroleum Geology, Core Conference CD Volume, 15 p.

Eliuk, L.S. and Levesque, R. 1989. Earliest Cretaceous sponge reef mound Nova Scotia shelf (Shell Demascota G-32). *In:* H.H.J. Geldsetzer, N.P. James and G.E. Tebbutt, (eds.). Reefs, Canada and Adjacent Areas. Canadian Society of Petroleum Geologists Memoir 13, p. 713-720.

EnCana Corporation. 2006. Deep Panuke Offshore Gas Development, Volume 2 – Development Plan. (Document No: DMEN-X00-RP-RE-00-0003 Rev. 01U), 313 pp. (available on the CNSOPB website, www.cnsopb.ns.ca).

Given, M.M. 1977. Mesozoic and Early Cenozoic geology of offshore Nova Scotia, Bulletin of Canadian Petroleum Geology, v. 25, p. 63-91.

Harland, N., Hogg, J., Riddy, R., Syhlonyk, G., Uswak, G., Weissenberger, J. and Wierzbicki, R**.** 2002. **(**abstract), A major gas discovery at the Panuke Field, Jurassic Abenaki Formation, offshore Nova Scotia**,** Canadian Society of Petroleum Geologists, Annual Meeting, Calgary, p. 154.

Kidston, A.G., Brown, D.E., Smith, B.M. and Altheim, B. 2005. The Upper Jurassic Abenaki Formation offshore Nova Scotia: a seismic and geologic perspective. Canada-Nova Scotia Offshore Petroleum Board CD publication , 168 p

Leinfelder, R.R. 1994. Distribution of Jurassic reef types: a mirror of structural and environmental changes during breakup of Pangea. *In:* A.F. Embry, B. Beauchamp, and D.F. Glass (eds.), Pangea: Global Environments and Resources, Canadian Society of Petroleum Geologists Memoir 17, p. 677-700.

Leinfelder, R.R. Schmid, D.U. Nose, M and Werner, W. 2002. Jurassic reef patterns – the expression of a changing globe, *In:* W. Kiessling, E. Flugel and J. Golonka (eds.), Phanerozoic Reef Patterns, SEPM Special Publication No. 72, p. 465-520.

McIver, N.L. 1972. Cenozoic and Mesozoic stratigraphy of the Nova Scotia Shelf, Canadian Journal Earth Sciences, v. 9, p. 54-70.

Scotese, C. R. 1997. Paleogeographic Atlas, PALEOMAP Progress report 90-0497, University of Texas at Arlington, 20 p.

Wade J.A. and MacLean B.C. 1990. Aspects of the geology of the Scotian Basin from recent seismic and well data. *In:* M.J. Keen and G.L. Williams Geology of the Continental Margin of Eastern Canada (eds.), Geological Survey of Canada, No. 2, Part 2, p. 190-238

Weissenberger, J. Harland, N. Hogg, J. and Syhlonyk**,** G. 2000. Sequence stratigraphy of Mesozoic carbonates, Scotian Shelf, Canada; GeoCanada 2000 Convention (CSPG-GAC etc. CD disk, 5 p.)

Weissenberger, J.A.W., Wierzbicki, R.A. and Harland, N.J. 2006. Carbonate sequence stratigraphy and petroleum geology of the Jurassic Deep Panuke Field, Offshore Nova Scotia, Canada. *In:* P.M. Harris and L.J. Weber (eds.), Giant Hydrocarbon Reservoirs Of The World: From Rocks To Reservoir Characterization And Modeling: AAPG Memoir 88/SEPM Special Publication, p. 395-431.

Welsink, H.J. Dwyer, J.D. and Knight, R.J**.** 1989. Tectono-stratigraphy of the passive margin off Nova Scotia, *In:* A.J, Tankard and H.R. Balkwill (eds.), Extensional Tectonics and Stratigraphy of the North Atlantic Margin, American Association Petroleum Geologists Memoir 46, p. 215-231.

Wierzbicki, R., Dravis, J.J., Al-Aasm, I., and Harland, N. 2006. Burial dolomitization and dissolution of Upper Jurassic Abenaki platform carbonates, Deep Panuke reservoir, Nova Scotia, Canada. American Association of Petroleum Geologists Bulletin, v. 90, p. 1843-1861.

Wierzbicki, R., Gillen, K., Ackermann, R., Harland, N., Eliuk, L. with a contribution by J.Dravis. 2005. (extended abstract), Interpretation of a Fractured Dolomite Core: Margaree F-70, Deep Panuke, Nova Scotia, Canada. Abstract and core conference article – CSPG-AAPG Convention June core conference in Calgary AB (25 pages on CD).

Wierzbicki, R. Harland, N. and Eliuk, L. 2002. (extended abstract.), Deep Panuke and Demascota core from the Jurassic Abenaki Formation, Nova Scotia: facies models, Deep Panuke, Abenaki Formation, Canadian Society of Petroleum Geologists Annual Meeting, Core Convention Extended Abstracts, p. 71-101.

Wierzbicki, R. and Harland, N. 2004. (extended abstract), Diagenetic Model: Deep Panuke Reservoir, Offshore Nova Scotia, Canada, American Association of Petroleum Geology, Annual Convention 2004, Dallas.

Yassir, N.A. and Bell, J.S. 1994. Relationships Between Pore Pressure, Stresses, and Present-Day Geodynamics in the Scotian Shelf, Offshore Eastern Canada. American Association of Petroleum Geology Bulletin. v. 78. p.1863-1880.

APPENDIX – Cores in Panuke PI-1A and H-08

Until the Margaree F-70 core, recovery of Abenaki Formation core in the Deep Panuke Field was very poor and necessitated the use of FMI (formation imaging logs) calibrated by drilled sidewall cores. Their locations in the southern Deep Panuke pool are shown in Figure 1A. Sidewall cores were also taken in Margaree F-70 and MarCoh D-41. The short whole cores are shown in Figures 2A (Panuke PI-1A) and 3A (Panuke H-08)

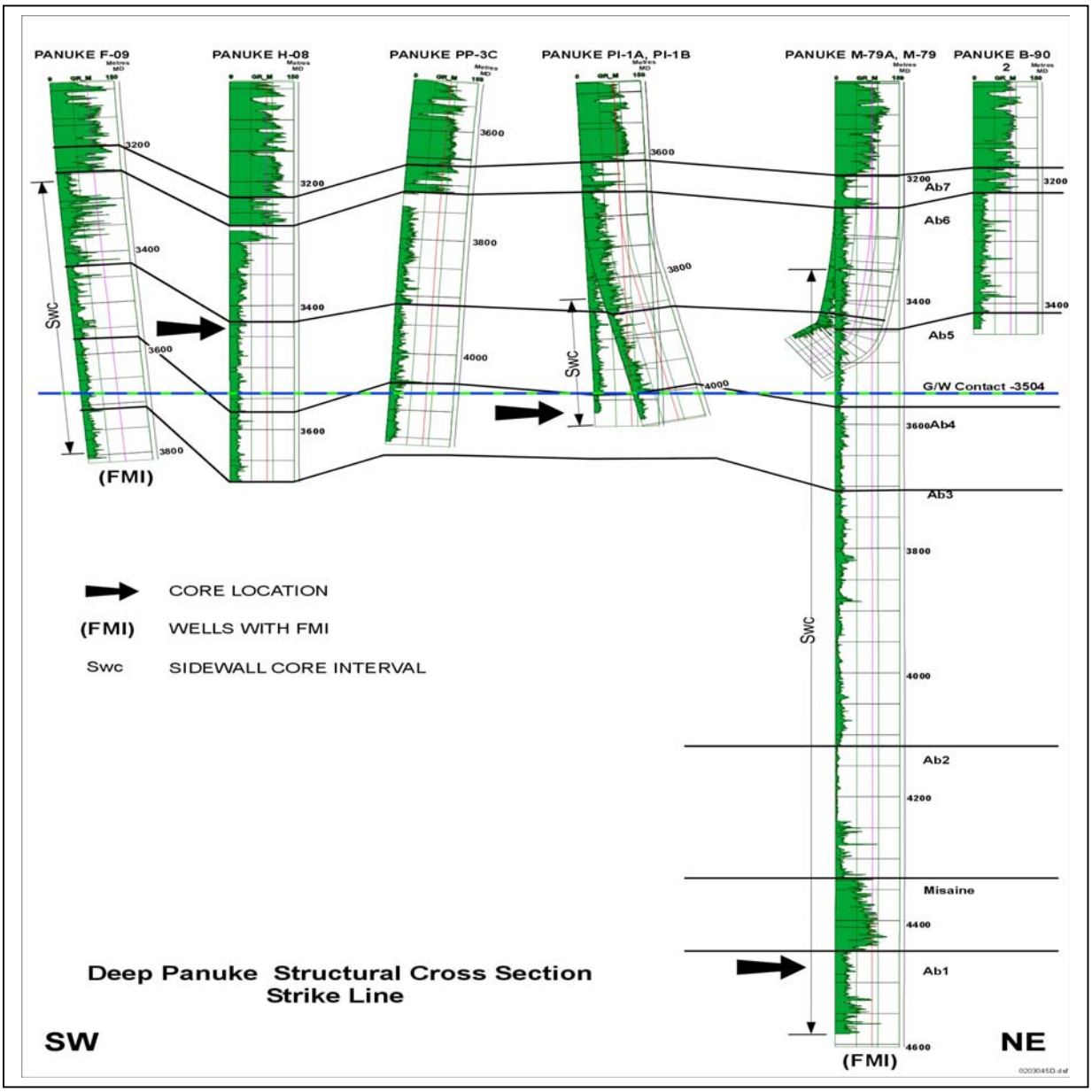

Figure 1A. Panuke wells gamma ray correlation section of sequences and distribution of cores (from Wierzbicki et al. 2002). There is a Scatarie Member (AB2) core in M-79.

Figure 2A. Panuke PI-1A core #1 – dolomite F-M crystalline with vuggy and intercrystalline porosity. Only 1.1 m recovered from 4029.28 m to 4032.8 m in AB 4.

Figure 3A. Panuke H-08 core #1 – limestone of upper chaetetid-rich (coralline sponge) bioeroded rudstones to floatstones with minor colonial corals and common echinoderm grain- to packstones as matrix and dominant in lower core. Limestone has high amounts of micro-porosity and some brecciation. About 3.2 m recovered in AB 5.

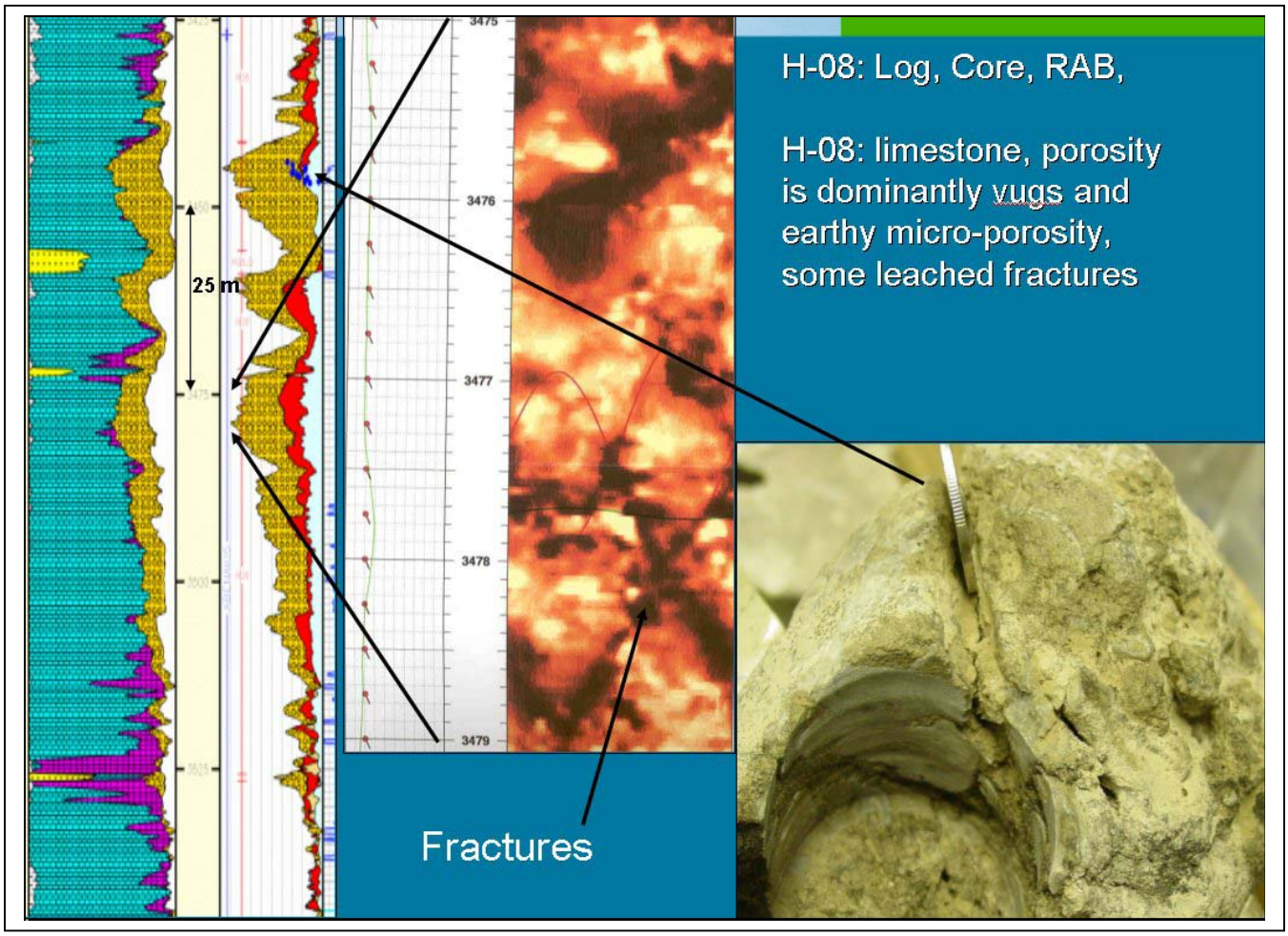

Figure 4A (Figure 7 of Wierzbicki et al. 2005): H-08 lithologic interpretation, RAB image shows fractures in well bore; core photo shows Canadian Toonie coin in open fracture.